2020 Building Performance Analysis Conference and
SimBuild co-organized by ASHRAE and IBPSA-USA

EFFECT OF GEOMETRY AND OPERATIONAL PARAMETERS OVER THE DEHUMIDIFICATION PERFORMANCE OF A DESICCANT COATED HEAT EXCHANGER

Ming Qu,[1] Thomas Pablo Venegas,[1] Kashif Nawaz,[2] and Lingshi Wang[2]
[1]Purdue University, West Lafayette, IN
[2]Oak Ridge National Laboratory, Oak Ridge, TN

ABSTRACT

Solid desiccant dehumidification systems are an alternative to dehumidification systems through condensation. They use solid desiccant materials to adsorb the moisture in the process air for space cooling. There are two configurations of the solid desiccant dehumidification system: desiccant wheels and desiccant coated heat exchangers (DCHE).

Previous studies focused on the effect on dehumidification performance using different desiccant materials on the DCHE. However, the performance of dehumidification remains to be quantified because the geometrical and operational conditions of the DCHE also play an essential role in its dehumidification performance for a given desiccant material. Therefore, it is important to evaluate their effects on dehumidification performance through modeling to assist in component design and operation. This paper provides the details of a one-dimensional heat and mass transfer model developed for this purpose. The model uses an implicit finite difference scheme to solve the governing equations, which represent the heat and mass balances in the control volume. The heat balances are evaluated for the airflow, water flow, tube, desiccant, and fin. The fin and solid desiccant are considered as having the same temperature. The mass balances are evaluated for the airside and the solid desiccant material. The outlet humidity results for dehumidification and regeneration showed a deviation lower than 15% from the experiment for most of the time. Still, the outlet temperature showed more difference, with results outside the 15% deviation range. The model temperature results also showed a faster change than the experiment. The model developed can be used to assist in the optimization of component design and operation for the best dehumidification performance.

INTRODUCTION

Air dehumidification is a common and important process in air conditioning. Air humidity affects human thermal comfort and health (ASHRAE, 2017). The process commonly used nowadays for dehumidification on commercial air conditioning systems is the undercooling of process air below its dew point, which produces the condensation of the air moisture. However, this process seriously undercools the air below comfortable supply temperatures, and therefore, a reheat process must follow the undercooling process. This process produces an energy expenditure in undercooling and in reheating, with only a fraction of it being used for actual dehumidification. Based on this situation, research has sought an alternative dehumidification process that does not rely on the cooling to the dew point of ventilation air. One promising alternative is the use of desiccant materials, that make use of the affinity of water molecules in the air, to remove those molecules to a different medium, and then supply the dehumidified air into the occupied rooms (Liu 2019). Among those technologies, the use of solid desiccant materials has attracted much research interest, and specially, the use of solid desiccant coated heat exchangers has received increasing attention in the last years, as the results published on Scopus of the number of publications, as shown in Figure 1.

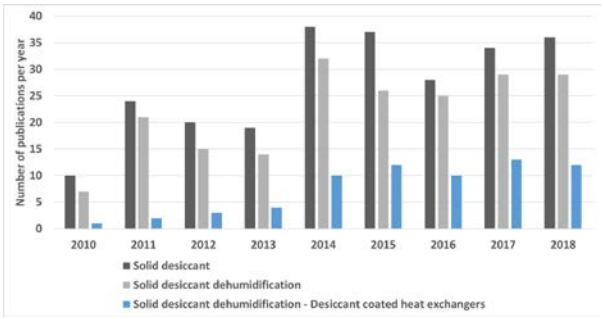

Figure 1 Publications on solid desiccant dehumidification collected in Scopus, accessed on 2019-11-05.

There are two common configurations of solid desiccant dehumidification systems: desiccant wheels (DW) and desiccant coated heat exchangers (DCHE) (Saeed and Al-Alili, 2017). In the DW process, air flows through desiccant coated channels where air moisture content is adsorbed. Meanwhile, one angular section of the rotating disk is performing a dehumidification process. Another section is being regenerated at the same time by the inflow of hot, dry air. DW mechanical configuration is relatively simple and can provide a continuous supply of dehumidified air. However, the use of DW has some drawbacks that limit its application. Because of the adsorption heat being released during the adsorption process, they tend not to be able to thoroughly saturate

the desiccant material (Vivekh et al. 2018). DW based-systems require of sensible cooling devices located downstream and in series with the DW (Nie 2017).

DCHE presents advantages over DW that explain the interest to study them. By being internally cooled, DCHE can reach higher desiccant saturation. Internal cooling also allows the DCHE to act over the sensible load of the process air, which for specific applications and DCHE design, may allow dispensing with auxiliary sensible cooling devices downstream from the DCHE. However, this comes at a cost. A DCHE cannot perform dehumidification and regeneration at the same time as a single DW unit can. To overcome this limitation, at least two units of DCHE should be placed in parallel, one performing dehumidification while the other is being regenerated.

Previous studies (Zheng et al. 2015, Zheng et al. 2016, Xu et al. 2019, Vivekh et al. 2019) evaluated the effect on dehumidification performance of using different desiccant materials on the DCHE. Operational parameters such as air velocity, water mass flow rate, and hot and cold water temperatures have been studied previously for given DCHE geometries and configurations (Hu 2015 et al., Xu 2019 et al., Jagirdar 2018 et al., Vivekh 2019 et al.). Decreasing water cooling temperature, and increasing regeneration water temperature was found to increase the amount of moisture removal by the DCHE (Hu 2015 et al., Vivekh et al. 2019, Xu et al. .2019). The air velocity and water mass flow rate were also found to have an impact over DCHE moisture removal, with lower velocity and higher water mass flow rates producing more moisture removal (Jagirdar et al., 2018). Design parameters such as fin pitch, external tube diameter, fin thickness, and solid desiccant thickness have been evaluated in previous works (Ge 2011 et al., Jagirdar 2018 et al., Vivekh et al. 2019). A decrease in fin pitch was found to increase moisture removal, although it increases the required fan power (Ge 2011 et al., Jagirdar et al., 2018). The effect of the external tube radius was studied (Ge et al. 2011), finding that by increasing the outer tube radius, it produced an increase in moisture removal. Different geometrical configurations of fin and tubes in the DCHE were evaluated (one tube row, two staggered tubes rows, three staggered tubes rows, and annular fins) (Vivekh et al., 2019). It was found that two staggered tubes and the use of annular fins produced higher moisture removal than the alternatives. The effect of increasing the desiccant layer thickness over mass transfer was evaluated (Jagirdar et al., 2018). An increase in the desiccant layer thickness increased moisture removal. However, it was only evaluated for their effect over the mass transfer and not its effect over heat transfer because a uniform fin and desiccant temperature has been assumed. Unlike the other parameters, it was found that varying the fin thickness did not produce significant changes in DCHE performance (Jagirdar et al., 2018). These studies show that the design parameters and operating conditions of the DCHE influence its performance. The parametric evaluation of operational variables shows that for a given DCHE design, optimization of operational parameters is required to ensure the highest possible moisture removal. Therefore, the adequate selection of desiccant material, design of heat exchanger, and selection of operational conditions are required processes to obtain the highest moisture removal from a DCHE device. Therefore, it is important to evaluate their effects on dehumidification performance through modeling to assist in component design and operation.

In this article, a model to simulate a section of a solid desiccant coated heat exchanger has been developed and compared to an experimental reference for validation. The model describes the heat and mass transfer phenomenon, which takes place inside a representative control volume of the heat exchanger. Following this study, the model will be expanded to represent the complete geometry of the desiccant coated heat exchanger. The paper presents the main assumptions, governing equations, validation process, and the performance-prediction of the model, as wells as shows the capabilities of it as a research and element design tool.

HEAT AND MASS TRANSFER 1-D MODEL OF DCHE

A desiccant coated heat exchanger (DCHE) is similar to a typical finned coil heat exchanger, but with a thin layer of solid desiccant coated on the surfaces of fins. Air crosses the largest face of the DCHE through the channels formed between the fins. Water flows inside the tube, which crosses the fins perpendicularly, describing a folded path with several passes crossing the main face of the DCHE.

Therefore, a DCHE can be described as having at least two scales of relevance for dehumidification, one representing the path of the air, and its residence time between the desiccant coated fins, and the other one for water.

A diagram of the cross-section of a DCHE, including several air channels between fins at the dehumidification stage, is shown in Figure 2. The model for the first scale is a 1-D model of the air channel between two fins. By assuming symmetry above for the air channel and below for the half of the metallic fin, this section includes half of one fin, its desiccant coating layer, and half of the air channel above it, as shown inside of the dashed box in Figure 2.

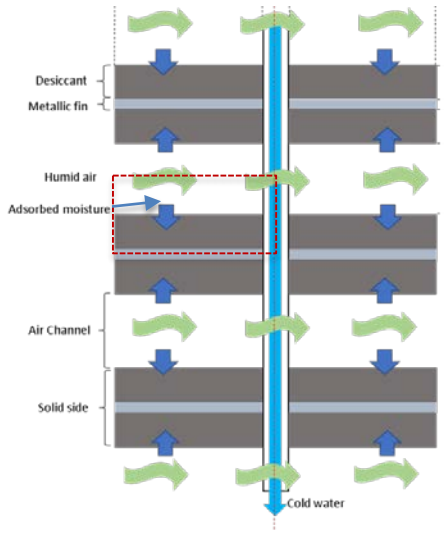

Figure 2 Air channels and fins in DCHE

The model for this scale represents the actual heat and mass transfer interactions between the solid desiccant and the air. Therefore, it must include the information regarding the adsorption process itself, such as the adsorption isotherm curve of desiccant material, heat of adsorption, convective heat, and mass transfer between solid desiccant and air. Between air and the desiccant layer, there is convection heat exchange. Heat is stored on the mass of the DCHE (desiccant layer, metallic fin, and water tube) and the moisture adsorbed by the desiccant. Between the exterior surface of the water tube and the desiccant and metallic fin section in contact with it, there is conduction heat transfer. Between the desiccant layer and fin elements located in different positions along the air channel, there is also conduction heat transfer. Finally, convection heat transfer takes place inside the tubes, which produces heat exchange between the water and the interior surface of the tube.

The model for the second scale represents the energy balance in 1-D for the two main elements of this scale, the water tube and the water itself. The water can supply or receive heat from the tube, while the tube stores part of that heat and transfer the rest by conduction to the fin elements and the next section of the tube. Therefore, in this direction, energy balances are calculated for the water and the tube. The heat transfer mechanism between the water and the tube is convection. Meanwhile, the heat transfer mechanism between the tube and the solid side of the fins is conduction. The water flow only acts as a heat sink or supply. Therefore there are no mass exchanges associated with this phase, and water mass is conserved along the vertical direction. Along the main direction of the 2nd scale, a sequence of fins and air channels is found. Then, to model the behavior of the DCHE in this scale, several iterations of the 1st scale 1D model can be called, changing the temperature conditions of the tube and water for each one, according to the energy balances on the elements of the 2nd scale.

There are several assumptions made to represent only the relevant factors for dehumidification or regeneration that take place in the control volume. The assumptions considered are the following:

1. Uniform distribution of fins and tubes in the DCHE.
2. The desiccant material and the metallic fin are at the same temperature.
3. Neither heat nor mass transfer exists on the Y direction for either desiccant or airstream.
4. The water and tube temperatures are uniform for each air channel segment.
5. Adsorption heat is released into the desiccant material only.
6. Both water and air move in one direction
7. No binder material is between solid desiccant and metallic fin.

By discretizing the air channel and solid side along the airflow path axis, two different control volumes are presented. The first one represents the unobstructed section, not in contact with the tube, and at the center of the air channel path, the control volumes would be in contract with the tube exchanging heat with it.

The governing equations for the energy balances of air, solid side, tube, and water are following.

Equation (1) shows the energy balance for the airflow. The first term on the left-hand side (LHS) represents the convective heat exchange between the air and solid desiccant, the following term represents the heat exchange present in the central elements between the exterior surface of the water tube and the air, the third term represents the temperature gradient along the airflow direction, and the term on the right-hand side (RHS) of the equation represents the change in temperature in time for a given cross-section of the air channel.

$$h_a \cdot L_y \cdot (T_d - T_a) + h_{aT} \cdot L_{za} \cdot (T_T - T_a) - u_a \cdot L_y \cdot L_{z,a} \cdot \rho_a \cdot Cp_a \cdot \frac{\partial T_a}{\partial x} = L_y \cdot L_{z,a} \cdot \rho_a \cdot Cp_a \cdot \frac{\partial T_a}{\partial t} \quad (1)$$

Equation (2) shows the energy balance on the solid side (solid desiccant and fin). The first term on the LHS represents the heat conduction between elements. The second term represents the heat gain due to the release of adsorption heat to the desiccant material. The third term represents the convective heat exchange between air and desiccant, while the fourth term only applies to the center

elements and represents the conduction heat exchange between the solid section (solid desiccant and fin) and the exterior face of the water tube. On the RHS, the term stands for the heat storage on the solid desiccant, fin and adsorbed moisture.

$$\left(k_d \cdot L_y \cdot L_{z,d} + k_f \cdot L_y \cdot L_{z,f}\right) \cdot \frac{\partial^2 T_d}{\partial x^2} + h_{m,a} \cdot L_y \cdot (w_a - w_d) \cdot \Delta H_{ads} - h_a \cdot L_y \cdot (T_d - T_a) - \left(\frac{k_d + k_f}{L_y}\right) \cdot \left(\frac{L_{zf} + L_{zd}}{L_y}\right) \cdot (T_T - T_d) = \left(\rho_d \cdot L_y \cdot L_{z,d} \cdot Cp_d + \rho_f \cdot L_y \cdot L_{z,f} \cdot Cp_f + \gamma_d \rho_w \cdot L_y \cdot L_{z,d} \cdot Cp_w\right) \cdot \frac{\partial T_d}{\partial t} \quad (2)$$

In Equation (3), the energy balance for the water tube is shown. The first term on the LHS represents the convective heat exchange between water and the interior surface of the tube while the second term represents the conduction heat exchange between the tube and the central elements of the solid side (solid desiccant and fin). The term on the RHS represents the heat stored on the analyzed section of the water tube.

$$h_w \cdot A_w \cdot (T_w - T_t) - \left(\frac{k_d}{L_y} \cdot L_{zd}\right) \cdot \left(\frac{k_f}{L_y} \cdot L_{zf}\right) \cdot (T_t - T_d) = (\rho_t \cdot A_t \cdot Cp_t) \cdot \frac{dT_t}{dt} \quad (3)$$

Following the approach by Jagirdar et al. (2018), the water-energy balance considers that the change of energy in the water flow is equal to the convective heat transfer between the water and the inner tube surface.

$$\dot{m}_w \cdot Cp_w \cdot (T_{wo} - T_{wi}) = h_w \cdot A_w \cdot (T_t - T_w) \quad (4)$$

On the LHS of Equation (5), the first term shows the convective mass transfer between solid desiccant and air, while the second term represents the gradient in moisture content along the airflow direction. On the RHS of the equation, the term describes the change in moisture content in time for a given element.

$$h_{m,a} \cdot L_y \cdot (w_d - w_a) - u_a \cdot L_y \cdot L_{z,a} \cdot \rho_a \cdot \frac{\partial w_a}{\partial x} = L_y \cdot L_{z,a} \cdot \rho_a \cdot \frac{\partial w_a}{\partial t} \quad (5)$$

Based on Ge et al. 2011, the first term on the RHS in Equation (6) represents the convective mass transfer between the solid desiccant and air, while the second term represents the change in adsorbed moisture on the solid desiccant.

$$h_{m,a} \cdot (w_a - w_d) - L_{z,d} \cdot \rho_d \cdot \frac{\partial \gamma_d}{\partial t} = 0 \quad (6)$$

An additional equation is required to solve the governing equations. This equation is the water adsorption isotherm curve of solid desiccant material. This equation must represent the water adsorption isotherm curve for the specific desiccant material used in the model.

For the validation procedure, the desiccant material used in the reference (Tu et al. 2017) has been implemented in the model. On the reference work, an empirical expression for the water adsorption isotherm curve is provided. Table 1 presents the water adsorption curve for different ranges of relative humidity, and Table 2 presents the relative humidity values for each section.

Table 1 Water adsorption isotherm for validation

SECTION	WATER ADSORPTION ISOTHERM
I:	$\gamma_d = 0.133 \cdot e^{(-1.12\times10^{-6}\cdot(-RT\cdot\ln(RH)))^{2.241}}$
II:	$\gamma_d = 0.224 - 0.0004 \cdot (RT \cdot \ln(RH))$
III:	$\gamma_d = 2.235 \cdot e^{(-0.472\cdot(-RT\cdot\ln(RH)))^{0.332}}$

Table 2 Ranges of relative humidity for water adsorption isotherm for validation

SECTION	RELATIVE HUMIDITY RANGE
I:	0% – 3%
II:	3% - 30%
III:	> 30%

Following, auxiliary equations for terms used in the governing equations are shown.

The Nusselt number used to calculate the convection heat transfer coefficient between air and desiccant is based on Ge et al. (2011), shown in Equation (7).

$$Nu_{ha} = 0.332 Re^{1/2} Pr^{1/3} \quad (7)$$

Convective heat transfer for the heat exchange between the water and air are based on the Nusselt number provided by Karava and Qu (2018), and shown in Equation (8).

$$Nu_{ha} = 0.683 Re^{0.466} Pr^{1/3} \quad (8)$$

Adsorption heat for the desiccant material used in the validation procedure is based on the value provided by Tu et al. (2017).

$$\Delta H_{ads} = 2662\ [kJ/kg] \quad (9)$$

The Nusselt number expression used to calculate the convective heat transfer between water and tube is based on Karava and Qu (2018), shown in Equation (10).

$$Nu_{hw} = \frac{\left(\frac{f}{8}\right)((Pr-1000)Pr)}{1+(12.7)\left(\frac{f}{8}\right)^{0.5}\left(Pr^{2/3}-1\right)} \quad (10)$$

$$f = \left((0.79 \cdot \log(Re)) - 1.64\right)^{-2} \quad (11)$$

Convection mass transfer coefficient between air and solid desiccant is calculated using Equations (12) and (13), by Ge et al. (2011).

$$h_{m,a} = \frac{\rho \cdot Nu \cdot D}{4 \cdot L_{zd}} \quad (12)$$

$$D = 0.00002302 \left(\frac{P_0}{101310}\right)\left(\frac{T_a}{256}\right)^{-2} \quad (13)$$

An implicit finite difference scheme has been used to solve the partial differential equations. The main boundary conditions are the inlet temperature and absolute humidity conditions of the airflow, which are constant for the complete time of the simulation. For the solid energy balance equation, a gradient of zero for heat conduction at the elements of the extremes is the boundary condition.

MODEL VALIDATION

The experimental work published by Tu et al. (2017) has been selected for model validation. The authors of the reference published their experimental evaluation of a DCHE along with a detailed spreadsheet of their experimental measurements of water inlet/outlet temperatures and air outlet temperature and humidity. The constructive characteristics of the DCHE of the experiments in the reference are listed in Table 3.

Table 3 DCHE design characteristics for validation

PARAMETER	VALUE
Air channel length	0.044 m
Air channel width	0.00675 m
Water-tube radius	0.00476 m
Air channel height	0.00105 m
Desiccant height	0.0002 m
Fin height	0.00015 m
Desiccant material	Composite LiCl 16%w on SG matrix
Desiccant density	800 kg/m^3
Desiccant specific heat	1200 J/kg
Desiccant thermal conductivity	5.27 W/mK
Desiccant max sorption capacity	0.55 kg/kg
Fins	Aluminum
Tube	Copper

For the validation, the input variables based on the data of the reference are implemented in the model. They include water inlet temperature, the geometric and physical properties of the DCHE, and its component materials. The operational conditions of the dehumidification process of the reference are in Table 4.

Table 4 DCHE operational characteristics for validation

PARAMETER	DEHUMIDIFICATION	REGENERATION
Air inlet temperature [C]	30	30
Air inlet absolute humidity [kg/kg]	0.01604	0.01604
Air speed [m/s]	1.54	1.54
Process time [s]	600	600
Initial moisture content on desiccant [kg/kg]	0.05	0.55
Initial desiccant temperature [C]	47	27

The simulation results have compared the outlet conditions of the experiment published, including air outlet temperature and air outlet absolute humidity.

In the experiments, both air and water conditions are measured each at one point both at the inlet and outlet of each fluid into the DCHE. The 1D model of the air path section represents the complete air channel length, for one half of each section between two fins, assuming symmetry, For the waterside, only one segment is included in the current 1D model formulation. The experimental results are measured at only one position downstream from the DCHE, measuring average conditions.

Since the experimental measurements of the reference represent average conditions, the inlet water temperature for the model has been adapted from the experimental values. The outlet conditions of a segment located at the center of the cross area of the DCHE are expected to be closer to the average measured conditions, than the outlet conditions of a segment located near either the beginning of or the end of the water tube path. For this center element, the inlet water temperature is expected to be at a value average between measured inlet and outlet temperatures. For the current formulation of the first scale model, only one water tube segment considered, which represents a small fraction of the water tube inertia. The experimentally measured DCHE contains the equivalent of 7888 modules of the first scale model. Therefore, the heat stored by the tube would be underestimated and consequently influence the amount

of heat transferred from the water. This situation is described in the analysis of the result of the validation of each cycle.

Figure 3 and 4 are the comparisons of the results of the model (continuous line) and the experimentally measured values (dashed lines).

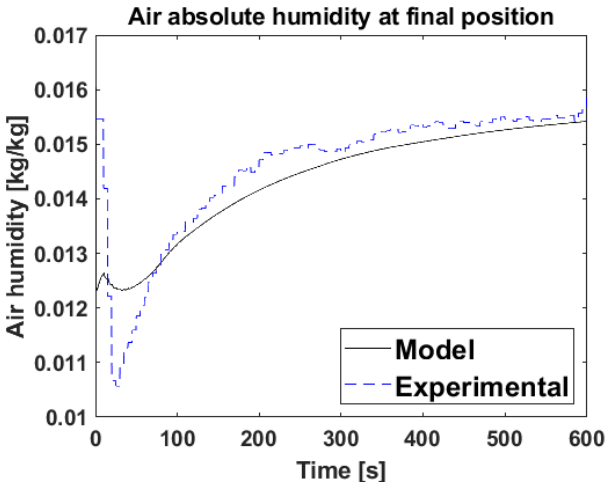

Figure 3. Dehumidification, air outlet absolute humidity

Figure 3 shows that beyond the initial 100 seconds, the results of absolute air humidity closely match the reference values both in absolute values and general curve behavior. The deviation from the experimental results for the initial 100 [s] is also present in the temperature results in Figure 4 below.

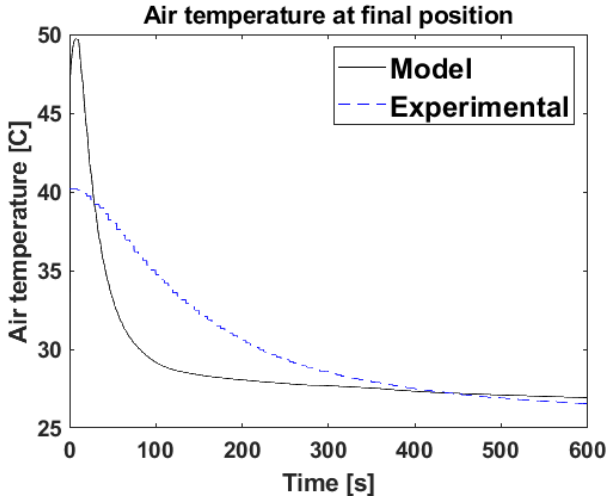

Figure 4. Dehumidification, air outlet air temperature

In Figure 4, the temperature results show a larger deviation from the experimental values, until close to 300 seconds. This deviation suggests a faster thermal response from the model than the measured values, due to a fast increase as the inlet water starts reducing its temperature until reaching the 25 [°C] used for dehumidification from the 50 [°C] used for regeneration, and also a faster decrease than the experiment until reaching temperatures close to 27[°C] after 100 [s]. It could be due to the lower thermal capacity present in the 1-D model, than what is expected of the complete DCHE.

Figure 5 and 6 show a comparison of the experimental and model values by providing a band of +15% to -15% deviation as reference for the exactitude of the model, as used by Ge et al. (2011).

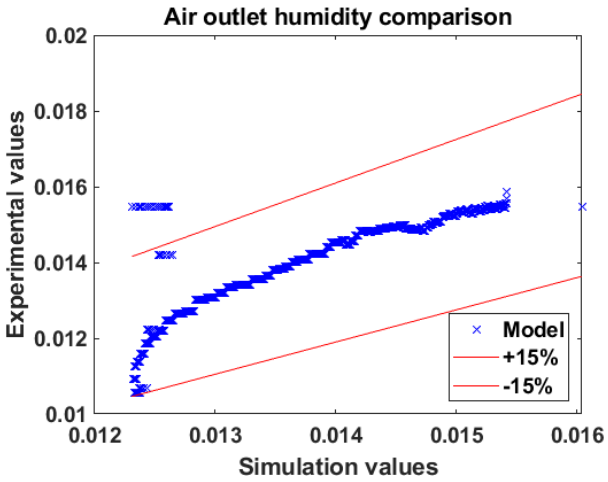

Figure 5. Dehumidification, air outlet absolute humidity

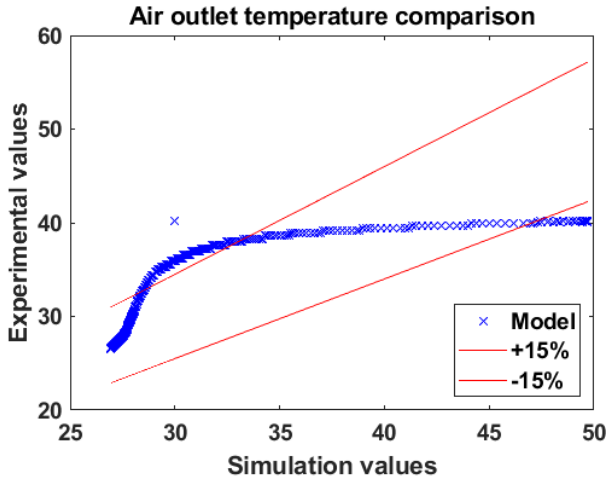

Figure 6. Dehumidification, air outlet air temperature

Despite the deviations shown for the initial 100 [s], the comparisons using the +15% to -15% deviation band show that a significant share of the model results is inside that band, providing evidence of the capabilities of the

model for describing the dehumidification process accurately.

Figure 7 and 8 show the results of the model simulation (continuous line) and the experimentally measured values (dashed lines) when the DCHE is operated in the regeneration stage.

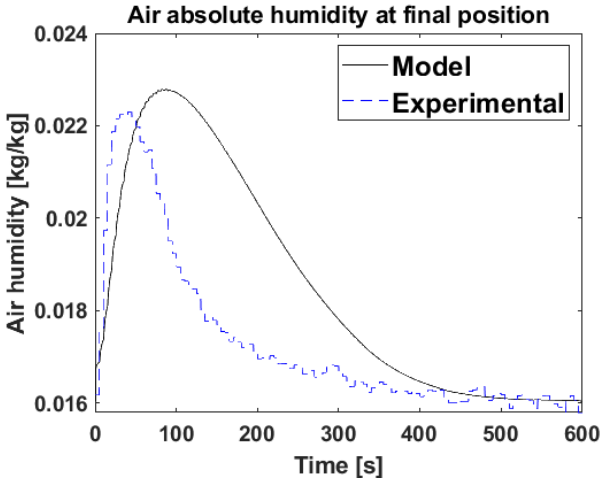

Figure 7. Regeneration, air outlet absolute humidity

The regeneration values from modeling results tend to be further away from the measured values than for the case of dehumidification. It can be influenced by the smaller thermal capacity of the model compared to the actual DCHE, and the larger temperature differences between water and solid phase that take place during regeneration, as compared to dehumidification. However, for absolute humidity, the model results are close in absolute values and curve behavior to the measured values, despite showing a lag in the time response.

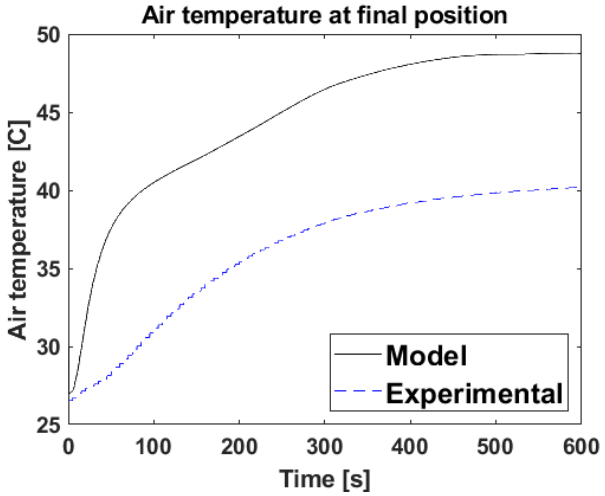

Figure 8. Regeneration, outlet air temperature

In the case of temperature shown in Figure 8, the faster response of the model to the temperature increase in water temperature is easily observable from the beginning of the process, and it remains significantly higher to the measured values for the complete regeneration process, even though the curve behavior is similar to the experimental results.

Figure 9 and 10 show a comparison of the experimental and simulated values for air absolute humidity and temperature, but providing a band of +15% to -15% deviation as reference for the exactitude of the model.

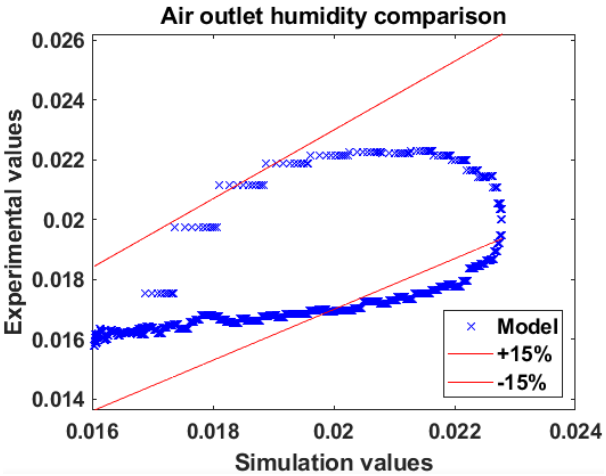

Figure 9. Regeneration, absolute outlet humidity comparison

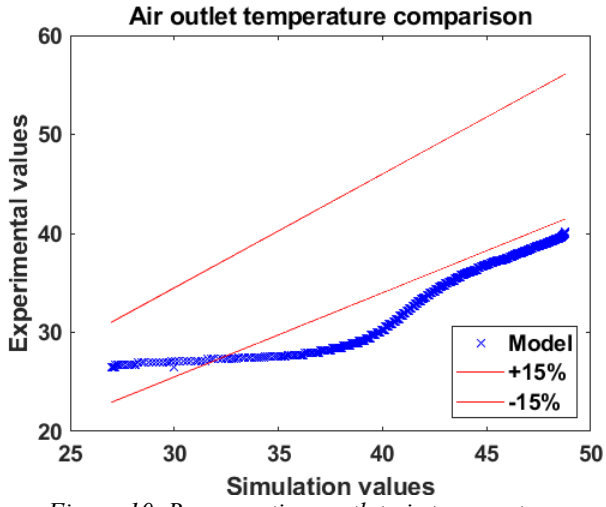

Figure 10. Regeneration, outlet air temperature comparison

As in the case of dehumidification, Figure 9 shows that the model results are in general inside the +15% -15% range from the experimental values, even though the model curve shows a slower decay of absolute air humidity than the experiment. Nevertheless, Figure 10 shows that the temperature values are outside the highlighted deviation range and specifically shows that

the model values are higher than the experimental values for a large fraction of the regeneration process, which can be related to the lower thermal capacity of the model than the experiment, which may cause that for the same heat flux input due to hot water flow, the model reaches higher temperatures.

DISCUSSION AND RESULTS ANALYSIS

The validation shows that the 1D model can accurately represent the air humidity at the outlet of the DCHE for both dehumidification and regeneration modes. The model can reproduce the general behavior of the change in time of absolute humidity of process air. The results for the regeneration process show a larger deviation from the experimental values, which can be explained by the differences between the model assumed average condition and experimental temperature behavior. However, the analysis of the deviations between experimental and model results for temperature suggests using a small segment of water tube for a significant effect over temperature. It is especially salient for the regeneration process, in which the larger temperature differences make even more evident this situation, with the model values not reaching the experimental values at the end of the 600s process, unlike dehumidification. Figure 4 shows this phenomenon clearly for the first 100 s of dehumidification, during which water starts flowing at 50°C influenced by the system thermal inertia and the recently finished regeneration process, producing a peak of the temperature of 49°C shortly after beginning the process, and as the water temperature falls, reaching a temperature close to the water inlet temperature (27°C) before 100°C while in the meantime the experimental results show a slower and steady decrease, reaching 27°C only at 400s of the dehumidification process. Figure 8 shows even more evidence of the influence of the differences in temperature behavior between the model and the experiment, showing a faster increase in temperature in the model than what showed in the reference, and maintaining though the complete regeneration process temperatures closer to the water temperature than what was measured in the experiment. The increase in temperature takes place before 100s, reaching 40°C from the initial 27°C and then maintaining a slower increase in temperature describing a behavior similar to the experiment. It is to be expected that by including more elements to the water tube while performing the second scale modeling, the temperature response of the DCHE would be slower, and therefore more closely match the experimental temperature values.

CONCLUSION

A 1-D finite-difference model has been developed to represent the heat and mass exchange phenomena in an air channel path of a DCHE. The model has been validated with experimental data from an existing reference. The experimental setup of the reference present differences with the model, so certain conditions are not directly comparable, but for the conditions that are more directly relatable (absolute air humidity), the results of the model show agreement with the experimental values. The results of air humidity tend to have a deviation of less than 15% as compared to the experimental values.

However, the validation process shows that only considering one tube segment has an important effect over air temperature. The model air temperature response tends to change faster than the measured values to the change in inlet water temperature. It is especially evident for the regeneration case, in which the higher temperature differences between the water and the air and solid phases of the model create larger deviations from the experimental results. To address this issue, an expansion of the model should include the effect of several sections of water tube, to increase the thermal capacity of the model, approaching the actual thermal capacity of the experimental DCHE, even though the experimental values are influenced by the thermal inertia of elements upstream and downstream of both air and water circuits, which are outside of the scope of the model.

ACKNOWLEDGMENTS

NOMENCLATURE

γ_d: Moisture load in desiccant[kg/kg]

w_a: Specific humidity in air [kg/kg]

w_d: Specific humidity in the air in desiccant pores [kg/kg]

T_a: Air temperature [K]

T_d: Solid temperature [K]

T_t: Tube temperature [K]

T_w: Water temperature [K]

$L_{z,a}$: Length of control volume on Z direction (air) [m]

$L_{z,d}$: Length of control volume on Z direction (desiccant) [m]

$L_{z,f}$: Length of control volume on Z direction (fin) [m]

L_y: Length of control volume on Y direction $[m]$

u_a: Air velocity $[m/s]$

ΔH_{ads}: Heat of adsorption $[J/kg]$

c: Separation factor [Dimensionless]

h_a: Convective heat transfer coefficient between air and desiccant $[W/m^2 \cdot K]$

ρ_a: Air density $[kg/m^3]$

$h_{m,a}$: Mass transfer coefficient $[kg/s \cdot m^2]$

RH_a: Relative humidity in air stream [Dimensionless]

$C_{p,a}$: Air specific heat $[J/K \cdot kg]$

k_a: Air thermal conductivity $[W/m \cdot K]$

k_d: Desiccant thermal conductivity $[W/m \cdot K]$

k_f: Fin thermal conductivity $[W/m \cdot K]$

$C_{p,f}$: Metallic fin Specific Heat $[J/K \cdot kg]$

$C_{p,d}$: Desiccant Specific Heat $[J/K \cdot kg]$

Pr_d: The porosity of the desiccant material [Dimensionless]

D_d: Mass diffusivity of desiccant material $[m^2/s]$

r_t: Water-tube radius $[m]$

$h_{a,Tub}$: Convective heat transfer coefficient between air and tube $[W/m^2 \cdot K]$

ρ_d: Desiccant density $[kg/m^3]$

ρ_f: Fin density $[kg/m^3]$

μ_{air}: Air kinematic viscosity $[kg/m \cdot s]$

REFERENCES

ASHRAE (2017). ASHRAE Standard 55 Thermal Environmental Conditions for Human Occupancy. Atlanta, USA: American Society of Heating Refrigerating and Air-Conditioning Engineers.

Ge, T. S. et al. (2011) Performance study of silica gel coated fin-tube heat exchanger cooling system based on a developed mathematical model. Energy Conversion and Management 52(6), 2329-2338.

Hu, L. M. et al. (2015) Performance study on composite desiccant material coated fin-tube heat exchangers. International Journal of Heat and Mass Transfer 90, 109-120.

Jagirdar, M. and Lee, P. S. (2018) Mathematical modeling and performance evaluation of a desiccant coated fin-tube heat exchanger. Applied Energy 212, 401-415.

Karava, P. Qu, M. (2018) Architectural Engineering, Purdue University, West Lafayette, Indiana, USA.

Liu, L. et al.(2019) Numerical investigation of mass transfer characteristics for the desiccant coated dehumidification wheel in a dehumidification process Applied Thermal Engineering 160, 113944.

Nie, J. et al. (2017) Theoretical modeling and experimental study of a thermal conditioning process of a heat pump assisted solid desiccant cooling system. Energy and Buildings 153, 31-40.

Saeed, A. and Al-Alili, A. (2017) A review on desiccant coated heat exchangers. Science and Technology for the Built Environment 23 (1), 136-150.

Tu, Y. D. et al. (2017) Comfortable, high-efficiency heat pump with desiccant-coated, water-sorbing heat exchangers. Scientific Reports 7.

Tu, Y. D. et al. (2017) Desiccant-coated water-sorbing heat exchanger: Weakly-coupled heat and mass transfer. International Journal of Heat and Mass Transfer 113, 22-31.

Vivekh, P. et al. (2018) Recent developments in solid desiccant coated heat exchangers – A review. Applied Energy 2018, 778-803.

Vivekh, P. et. al. (2019) Theoretical performance analysis of silica gel and composite polymer desiccant coated heat exchangers based on CFD approach. Energy Convesions and Management 2019 (187) , 423-446.

Xu, F. et. al. (2019) Analysis on solar energy powered cooling system based on desiccant coated heat exchanger using metal-organic framework. Energy 2019 (117), 211-221.

Zhai, C. et al. (2008) Performance modeling of desiccant wheels (1): Model development. Proceedings of Energy Sustainability 2008 2, 209-2019.

Zheng, X. et al. (2014) Recent progress in desiccant materials for solid desiccant cooling systems. Energy 2014 (74), 280-294.

Zheng, X. et al. (2016) Experimental study and performance prediction of carbon based composite desiccant for desiccant coated heat exchangers. International Journal of Refrigeration, 2016 (72), 124-131.